Waste Management 120 (2021) 136–145

Contents lists available at ScienceDirect

Waste Management

journal homepage: www.elsevier.com/locate/wasman

Separation and concentration of valuable and critical materials from wasted LEDs by physical processes

Marcelo Pilotto Cenci *, Frederico Christ Dal Berto, Priscila Silva Silveira Camargo, Hugo Marcelo Veit

LACOR, Department of Materials Engineering, Federal University of Rio Grande do Sul (UFRGS), Av. Bento Gonçalves 9500, Porto Alegre, Brazil

ARTICLE INFO

Article history:
Received 11 May 2020
Revised 30 July 2020
Accepted 18 November 2020

Keywords:
LED
Electrostatic separation
Material concentration
Recycling
Gold
Gallium

ABSTRACT

The generation of wasted LEDs is expected to grow in the coming years, raising the challenge of recycling and recovering their valuable and critical materials. Due to the low concentration of these materials, the current recycling processes available for LEDs have a significant recovery limitation. This study proposes an innovative, clean and effective physical method to segregate the valuable and critical materials into different fractions while enhancing their concentration: particle size separation followed by electrostatic separation. After the determination of the best electrostatic separation conditions (varying tension and rotation) for each particle size, the final fractions were characterized by acid digestion and ICP-OES analysis. The analysis revealed that the economically valuable elements gold, silver, copper and tin became concentrated in the conductive fractions (80.18%, 94.22%, 96.55% and 93.29% of their total recovered mass, respectively), while the strategic critical elements, gallium, cerium and yttrium became concentrated in the non-conductive fractions (96.15%, 100% and 95.20% of their total recovered mass, respectively). Despite some limitations imposed by the mass losses, this novel route may be important to uncover new recycling alternatives, mainly for critical elements, and to improve the economic viability of the recycling routes.

1. Introduction

The Nobel Prize in Physics of 2014 was awarded to Isamu Akasaki, Hiroshi Amano and Shuji Nakamura for "the invention of efficient blue light-emitting diodes (LEDs) which has enabled bright and energy-saving white light sources" (Gayral, 2017). Since this invention and the insertion of white LEDs into the market, LEDs are continuously replacing conventional light sources, and are expected to reach 64% of the lighting market share in 2020 (Zissis and Bertoldi, 2018). Indeed, the higher energy efficiency, associated with the economic benefits and lower environmental impact, compared with conventional light sources, has made international organizations and many countries promote the use of LED sources by actions such as marketing, replacement campaigns and regulations (UNEP, 2017).

Due to the massive insertion of the LEDs in the market, LEDs are expected to contribute a large stream of Waste Electric and Electronic Equipment (WEEE) (Ogunseitan et al., 2009; Zhan et al., 2015), requiring management efforts to deal with it. Thus, as well as for other WEEEs, circular economy (CE) strategies must be applied to LEDs to reduce the associated environmental burden and to maximize the efficiency in the use of resources (Dzombak et al., 2019). CE aims to transform our economy into circular models in which wastes are minimized and are considered resources when generated. Such an approach in the management of WEEE is encouraged by the European Commission (2020), which proposed an action plan to promote the CE in order to achieve a sustainable future. CE also addresses many goals of the 2030 Agenda for Sustainable Development, proposed by the United Nations, in particular the target 12.5, which aims to reduce the waste generation through prevention, reduction, repair, reuse and recycling (Baldé et al., 2017).

Recycling is one of the main tools in the transition of our economy to a CE, aiming to close the loop between the generated waste and raw materials. Especially for WEEE, recycling plays an important role by minimizing the environmental pollution from discarded WEEE, reducing the demand for primary ores, and recovering critical and valuable materials back to the economy (Clarke et al., 2019; Grigoropoulos et al., 2020; Işıldar et al., 2018). In the context of CE, LEDs have been studied and considered as hazardous waste due to exceeding toxicity regulation standards for some metal concentrations (Kumar et al., 2019; Lim et al., 2011). However, they also contain valuable and critical materials

* Corresponding author.
E-mail addresses: marcelo.cenci@ufrgs.br (M.P. Cenci), dal.berto@ufrgs.br (F.C. Dal Berto), priscila.silveira@ufrgs.br (P.S.S. Camargo), hugo.veit@ufrgs.br (H.M. Veit).

https://doi.org/10.1016/j.wasman.2020.11.023
0956-053X/

to be potentially recycled, such as gold, silver, gallium, and rare earth elements (REE) (Cenci et al., 2020a; European Commission, 2018). Such characteristics and materials make the LEDs a target WEEE for recycling studies (Fang et al., 2018).

1.1. Brief context of LEDs composition and recycling

An LED is a complex assembly of optical, electrical, mechanical and thermal components. The constituent materials are variable and dependent on the manufacturer and technology advances (Franz and Wenzl, 2017). A scheme of a white LED with its main components is shown in the Fig. 1.

The working principle of the LEDs is through a sandwich of p-type and n-type semiconductor diodes (called chips) which emit light when an electric field is applied (Murali et al., 2015). The most efficient and successful approach to manufacture white LEDs is through gallium nitride (GaN) chips (layers of GaN above an alumina (Al_2O_3) base). The blue light emitted by the chips is converted into the visible spectrum by a phosphor light converter (Cho et al., 2017). The casing involving the chip is filled with silicon or epoxy resin containing the phosphor light converter, which is made of yttrium–aluminum garnet doped with cerium ($Ce:Y_3Al_5O_{12}$) (David and Whitehead, 2018; Feezell and Nakamura, 2018). Gold and silver are mainly used as electrical contacts and solders, and other metals such as copper, tin and aluminum are also applied to mechanical, thermal, and electrical purposes. (Franz and Wenzl, 2017).

As discussed, LEDs contain economically valuable metals (such as gold, silver, and copper) and strategic critical metals (such as gallium and REEs), and both of them are prospective targets for recycling initiatives. Reuter and Van Schaik (2015) simulated and optimized recycling routes for LED lamps, utilizing current available technologies of metallurgical extraction. In these simulations, gallium and REEs were lost, not being able to be recovered due to their low concentration and the applied technologies (mainly copper smelting). These simulations revealed the need for new recycling alternatives for LEDs, focusing on these critical elements. Indeed, Ueberschaar et al. (2017) reported that current WEEE recycling processes do not recover gallium and indicated the necessity of previous processes to segregate and concentrate the gallium in order to allow its recovery. In addition, Zhang et al. (2017) reported difficulties in recycling REEs due to their low concentration in WEEE, which is the case in LEDs, and highlighted the need for economic viability in the recycling processes.

A few studies have proposed specific recycling routes for LEDs. Murakami et al. (2015), Nagy et al. (2017) and Ruiz-Mercado et al. (2017) proposed hydrometallurgical routes to extract and recover, respectively, gold, gallium and REEs. Zhan et al. (2015) studied pyrolysis (as a step for material concentration) followed by vacuum metallurgy separation to recover gallium and indium. Zhou et al. (2019) studied a recycling route for gallium in which the LEDs were leached with organic acids, after a pyrolysis process to enhance the gallium concentration.

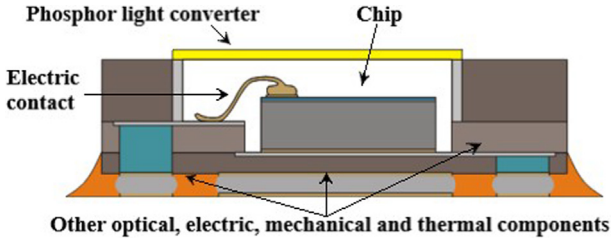

Fig. 1. Scheme of a white LED. Adapted from Deubzer et al. (2012).

The above-cited authors used acid digestion or pyrolysis as the primary step of the recycling routes. Such processes are related to the generation of hazardous effluents and emissions, and high energy consumption (Ilankoon et al., 2018). Ideally, the recycling processes should be as less polluting as possible since of the main recycling advantages is the minimization of the environmental burden. Additionally, the mentioned studies focused on recycling routes for specific metals (such as for gold, gallium or REEs), and previous steps to concentrate the materials were usually required. Thus, there is a limitation in addressing all the LED's valuable and critical materials that could be recycled.

A research gap was identified in efficiently segregating the valuable and critical LED materials into different flows, in order to allow and to maximize the recovery of such materials and make the recycling more profitable. Particularly, gallium and REEs should be segregated from the other materials such as gold and copper. This segregation is important to concentrate the materials and to allow the application of different recycling strategies for each flow (Ueberschaar et al., 2017). Such a novel approach may be useful to improve the current available recycling routes, and to even uncover new recycling alternatives. Physical processes for segregation and concentration are highly recommended due to the positive aspects concerning economic benefits, energy use, and generation of waste and effluents (Zhang and Xu, 2016). However, attention must be paid to the mass losses which are expected to be high in the physical processes (Kaya, 2016; Schneider et al., 2019).

Aiming to fill this gap, this study proposes the novelty of segregating and concentrating the valuable and critical LED materials into different fractions, by particle size and electrostatic separation. Thus, the critical elements can be processed by different recycling methods to the economically valuable elements. This novel approach for LEDs may be valuable as an initial step of a recycling route, before the traditional hydrometallurgical and pyrometallurgical steps. The expected superiority of the electrostatic separation over other physical methods for segregating LED materials, is due to the nature of the materials found in the LEDs in which valuable metals are found in the metallic form (metallic bonds), and critical metals in non-metallic form, so facilitating the segregation. Metals such as gold, tin, silver and copper are mainly used for electrical connection, soldering, and heat dissipation (Franz and Wenzl, 2017), being expected to fall into the conductive fraction (C) of the electrostatic separation. In contrast, the elements gallium and REEs are expected to fall into the non-conductive fraction (NC) since the gallium is used as gallium nitride (GaN) semiconductor, and the REEs are used in light converting materials ($Y_3Al_5O_{12}$ doped with Ce), mixed in a polymeric substrate (Cho et al., 2017; Feezell and Nakamura, 2018). The electrostatic separation, using a corona electrode, is the most effective method to separate conductive and non-conductive materials, and the current industrial processes may reach an efficiency of 95–99% of purity (Kaya, 2016). However, there are still efforts in new studies about electrostatic separation, with the focus on the optimization of the process and on the application of different WEEE (Hadi et al., 2015).

2. Materials and methods

Approximately, 5,500 LED units were manually collected from 62 LED tubular lamps of six different brands, obtaining 122 g to be further processed in the trials. A flowchart of the methodology adopted in the study is shown in Fig. 2.

2.1. Milling and particle size separation

After manual collection, the LEDs were milled in a knife mill until 100% passed through 1 mm. The particle size separation

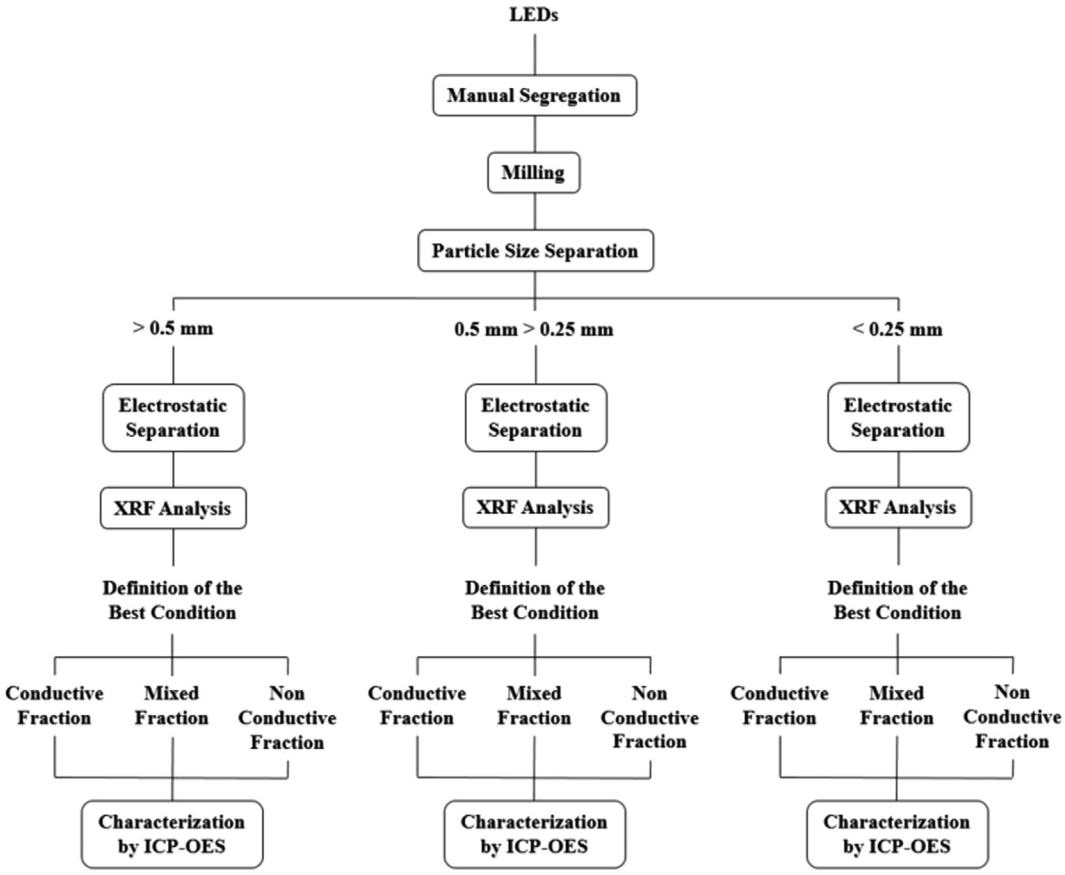

Fig. 2. Scheme of the methodology of the study.

was performed using bench sieves and an automatic agitator. The resultant material was divided into three fractions: above 0.5 mm (>0.5), between 0.5 mm and 0.25 mm (0.5 > 0.25) and below 0.25 mm (<0.25). These size fractions were selected due to the mass distribution of the resultant milled LEDs. The three fractions must have sufficient mass to perform the posterior experiments of electrostatic separation and characterization. These particle sizes are also intuitive and common for bench sieves and milling equipment, facilitating their reproducibility. The fractions had their mass measured and were sent to the electrostatic separation step.

2.2. Electrostatic separation

The experiments were performed in a corona-electrostatic separator (brand Inbras-Erieg, model ESP-14/01S). A schematic description of the separator and its electrode system is provided in Fig. 3.

The corona-electrostatic separation aims to segregate materials according to their conductivity. The particles are introduced to the system roll by an automatic vibratory feeder, and the roll is subjected to a high voltage electrostatic field by the corona electrode. The non-conductive particles become charged and remain attached to the surface of the roll, then fall into the NC fraction. The conductive particles are quickly discharged to the grounded roll and are attracted to the static electrode, falling into the C fraction (Kaya, 2016).

The fixed electrode system (angles and distances of the electrodes) used in the study was the same as adopted by Veit et al. (2005), Yamane et al. (2011) and Hamerski et al. (2018), which used similar equipment to process printed circuit boards (PCBs),

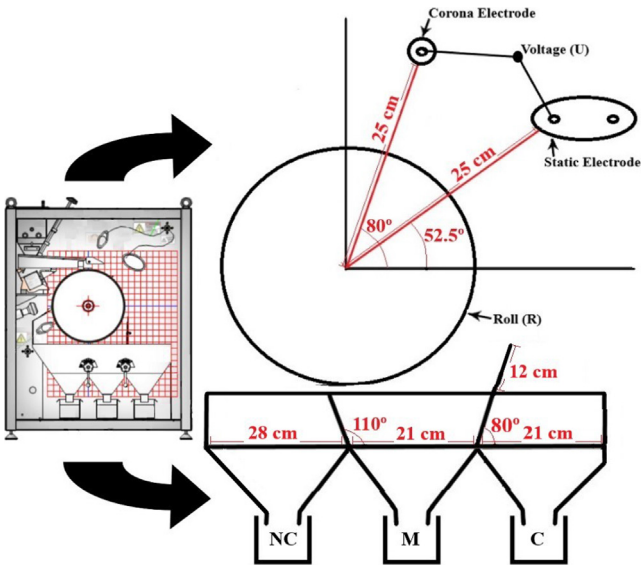

Fig. 3. Scheme of the corona-electrostatic separation.

with similar particle sizes. No studies were found on the application of electrostatic separation in LEDs. The electrode system adopted, illustrated in Fig. 3, is: corona electrode (angle from the horizontal axis: 80°; distance from the center of the roll: 25 cm) and static electrode (angle from the horizontal axis: 52.5°; distance from the center of the roll: 25 cm). The angles and dimensions of the collector are also illustrated in Fig. 3.

Before the electrostatic separation, the samples were dehumidified in a drying oven for three hours, at 100 °C, and the environment of the experiment room was controlled to keep humidity below 45%. For each particle size (>0.5, 0.5 > 0.25 and < 0.25), different voltages (U) and different roll rotations (R) were tested, in order to find the best condition of electrostatic separation. The conditions tested were: U = 20, 27 and 35 kV, and R = 30, 60 and 90 rpm.

In order to examine the performance of the conditions, the resultant non-conductive, mixed (M), and conductive fractions (of each varied condition) had their masses measured and were subsequently analyzed by X-ray fluorescence spectroscopy (XRF) in triplicate, to determine the metal concentration. A high metal concentration is expected in the conductive fraction and a low metal concentration in the non-conductive fraction. XFR analysis is useful to analyze the total elemental composition of samples (providing simultaneous analysis of several metals), being fast and non-destructive (Hunt and Speakman, 2015; Radu and Diamond, 2009). For individual elements, XRF analysis may not be a substitute for a more precise analysis, such as ICP-OES (Hunt and Speakman, 2015). Thus, XFR is used to approximate the total metal concentration of the fractions generated by electrostatic separation, and ICP-OES is used for further analyze the individual metals in the final fractions with the required precision.

To support the decision of the best separation condition, the statistical tests for means comparison, One-Way ANOVA, Fisher LSD (parametric tests) and Kruskal-Wallis (non-parametric test), were used at the confidence interval of 95%. These tests may be used to compare several independent samples (Hoffman, 2019). In this study, the tests were used to compare the average metal concentration of each resultant fraction for each condition (varying U and R). The normality test of Shapiro-Wilk and the variances' homogeneity test of Levene were used to identify which test should be applied (parametric or non-parametric). If the data distribution shows normality and homogeneity of variances, the parametric tests are used. If not, the non-parametric test must be applied (Heiberger and Holland, 2009; Hoffman, 2019; Scheff, 2016). The statistical tests were performed using the software Origin Pro 2016 and Minitab 17. A supplementary material, attached to this article, is provided to inform how the tests work, and their results.

Thus, as can be seen in Fig. 2, for each particle size, the best condition of electrostatic separation was determined and their resulting fractions were characterized by acid digestion followed by ICP-OES analysis. By this characterization, the separation, and the concentration of materials in each fraction, can be evaluated.

2.3. Characterization of the resultant best condition's fractions

In the characterization study of Cenci et al. (2020b), gold, silver, copper and tin were the main valuable elements found in LEDs, and gallium, cerium and yttrium the critical elements. Additionally, the critical elements indium, cobalt and antimony were also considered since they were found in other previous studies (Kumar et al., 2019; Rebello et al., 2020; Zhan et al., 2015).

The acid digestion was carried out with aqua regia (analytical-grade acids, 50 mL of acids for each gram of solids, 1:50) for two hours at 90–100 °C, and agitation speed between 300 and 400 rpm. To determine the amount of the silver element, the aqua regia was replaced by nitric acid (analytical-grade) under the same conditions, in order to avoid $AgCl_{(s)}$ precipitation (Petter et al., 2014). The resultant liquors were analyzed by ICP-OES.

For the characterization of the element gallium, a particular procedure was necessary due to the gallium nitride (GaN) refractory characteristics. GaN is a semiconductor used in the chips of the LEDs, which cannot be dissolved by chemical leaching (Zhuang and Edgar, 2005). A procedure proposed by Swain et al. (2016, 2015b, 2015a) and Nagy et al. (2017) was adapted and utilized in order to convert the GaN into leachable materials.

The solid material, collected by filtration after the aqua regia digestion, was processed in a tubular furnace with Na_2CO_3 (mass ratio 1:1) inside an alumina crucible, for eight hours at 1250 °C, in an air atmosphere. After the tubular furnace step, the material was acid digested in aqua regia (50 mL) for six hours at 90–100 °C, with an agitation speed between 300 and 400 rpm. The liquor was analyzed by ICP-OES.

3. Results and discussion

3.1. Milling and particle size separation

The milling step is essential to release the encapsulated materials from the LEDs, being necessary as a pretreatment before the electrostatic separation. The particle size separation may be important to determine the different best electrostatic separation conditions for each fraction, because particle size affects the electrostatic separation (Richard et al., 2017). Additionally, the particle size separation may concentrate some materials in its fractions.

The milling and the particle size separation generated three fractions: >0.5 (30.03 g), 0.5 > 0.25 (27.81 g) and < 0.25 (57.90 g). The mass loss during these steps was 5.13%.

3.2. Electrostatic separation

The fractions were processed in the corona electrostatic separator in order to determine the best separation condition varying U (20, 27 and 35 kV) and R (30, 60 and 90 rpm). It is important to highlight that the metal concentration results, given by the XRF analysis, are only used to determine the best separation conditions. The characterization of the final fractions was made by acid digestion and ICP-OES analysis, as can be seen in section 2.3.

In Table 1, the electrostatic separation results, of the particle size > 0.5, are shown. The table shows the XRF metal concentrations, their standard deviation, the resultant mass fractions, and the mass loss of each condition.

The conditions in U20 resulted in all the material falling into the conductive fraction. In U20 conditions, the electrostatic separation was not effective due to the low applied voltage for the relatively large particle size > 0.5. The material was directly thrown into the conductive collector by the centrifugal force of the roll rotation. Thus, the results of metal concentration were just repeated.

Initially, the conditions U27 R30, U27 R60, U35 R30 and U35 R60 had the best results. The statistical tests were used to support the determination of the best condition (results can be seen in the attached supplementary material). For the statistical tests and also for the posterior characterization, the M fraction was mixed with the NC fraction due to the similar concentrations (indeed in some conditions the M fraction has a lower metal concentration).

According to the ANOVA test for the C fraction, the conditions U27 R30, U27 R60, U35 R30 and U35 R60 are statistically identical (probability value of 0.082 at the 0.05 level). For the NC fraction, the Kruskal-Wallis's test informed that the conditions U27 R30, U27 R60, U35 R30 and U35 R60 are also identical (probability value of 0.644 at the 0.05 level). Thus, between these four identical conditions, the separation condition U27 R60 was chosen as the best due to the lower mass loss (0.85%). The results of the particle size 0.5 > 0.25 are shown in Table 2.

Similar to the particle size > 0.5, the conditions in U20 were not effective and the best separation conditions of the particle size 0.5 > 0.25 were initially U27 R30, U27 R60, U35 R30 and U35 R60, and the M fraction was mixed into the NC fraction. The

Table 1
Electrostatic separation results of the particle size > 0.5.

Conditions	Metal Concentration, %			Mass Distribution, %			Mass Loss (%)
	Conductive	Mixed	Non Conductive	Conductive	Mixed	Non Conductive	
U20 R30	35.69 ± 4.16	–	–	100	0.00	0.00	0.55
U20 R60	35.69 ± 4.16	–	–	100	0.00	0.00	0.49
U20 R90	35.69 ± 4.16	–	–	100	0.00	0.00	0.48
U27 R30	85.19 ± 5.04	2.56 ± 1.04	5.44 ± 0.60	84.05	13.67	2.28	1.67
U27 R60	89.11 ± 4.45	2.59 ± 1.07	4.46 ± 0.56	84.14	13.57	2.29	0.85
U27 R90	47.37 ± 6.51	7.55 ± 0.94	–	96.97	3.03	0.00	0.57
U35 R30	94.13 ± 2.10	2.32 ± 0.50	2.77 ± 0.01	84.38	5.41	10.21	3.87
U35 R60	95.00 ± 1.57	2.67 ± 0.36	2.14 ± 0.12	84.47	4.66	10.87	3.13
U35 R90	74.11 ± 8.03	2.31 ± 0.58	3.78 ± 0.16	86.16	13.68	0.16	3.08

U – Voltage; R – Rotation.

Table 2
Electrostatic separation results of the particle size 0.5 > 0.25.

Conditions	Metal Concentration, %			Mass Distribution, %			Mass Loss (%)
	Conductive	Mixed	Non Conductive	Conductive	Mixed	Non Conductive	
U20 R30	24.83 ± 1.27	11.44 ± 1.14	–	74.71	25.29	0.00	2.22
U20 R60	19.11 ± 1.75	54.02 ± 4.08	–	98.84	1.16	0.00	0.57
U20 R90	18.81 ± 2.30	10.76 ± 2.27	–	97.67	2.33	0.00	0.57
U27 R30	92.15 ± 2.72	11.48 ± 0.79	11.07 ± 2.00	26.38	35.58	38.04	2.30
U27 R60	92.08 ± 1.49	5.88 ± 1.10	7.48 ± 1.07	28.75	36.87	34.38	3.53
U27 R90	83.95 ± 4.38	8.69 ± 0.97	10.69 ± 0.61	22.29	77.07	0.64	1.83
U35 R30	93.91 ± 0.80	14.81 ± 1.68	7.31 ± 0.41	23.33	18.66	58.00	6.43
U35 R60	92.38 ± 0.63	21.44 ± 3.44	3.90 ± 0.41	25.69	10.42	63.89	6.88
U35 R90	75.54 ± 4.49	3.57 ± 0.33	2.28 ± 0.18	33.08	48.12	18.80	3.36

U – Voltage; R – Rotation.

ANOVA test for the fraction C, resulted in similarity between the four conditions tested (probability value of 0.656 at the 0.05 level). According to the ANOVA and Fisher's LSD tests applied to the NC fraction, the best separation conditions were U27 R60 and U35 R60, with the lowest (and similar) metal concentrations (probability value of 0.629 at the 0.05 level). Thus, the condition U27 R60 was chosen as the best between the two identical conditions, due to the lower mass loss (3.53%).The complete analysis can be seen in the supplementary material. Table 3 shows the results of the particle size < 0.25.

The electrostatic separation of the particle size < 0.25 resulted in a higher metal concentration in the NC fraction and higher mass losses, compared with the other particles sizes. The substantial mass losses, in the particle size < 0.25, may be a limiting factor for industrial scale processes. The U35 R90 condition was considered the best separation condition due to the lower metal concentration in the NC fraction (11.87%), and the metal concentration close to 90% of the C fraction, without the need for statistical tests support. For the subsequent characterization of the resulting fraction, the M fraction was mixed into the C fraction due to its small mass fraction (3.54%).

The resulting best separation conditions were: U27 R60 (for the fractions > 0.5 and 0.5 > 0.25) and U35 R90 (for the fraction < 0.25). Samples of the final fractions (C and NC of each particle size) were sent to acid digestion and ICP-OES analysis for characterization.

3.3. Characterization of the resultant fractions

After the processes of physical separation, the materials became segregated and concentrated by different particle sizes and electrostatic behavior. Table 4 presents the characterization of the C and NC fractions of each particle size, and the mass distribution of the elements between the final fractions.

Firstly, the results provided in Table 4 (characterized by ICP-OES) support and corroborate the XRF results of the electrostatic separation fractions. The particle sizes > 0.5 and 0.5 > 0.25 have similar metal concentrations in both the ICP-OES analysis (approximately 99% for the C fractions and 3% for NC fractions) and in the XRF analysis (approximately 90–92% for C fractions and 4–7% for NC fractions). The particle size < 0.25 has a higher metal concentration in the NC fraction than the other particle sizes, in both the

Table 3
Electrostatic separation results of the particle size < 0.25.

Conditions	Metal Concentration, %			Mass Distribution, %			Mass Loss (%)
	Conductive	Mixed	Non Conductive	Conductive	Mixed	Non Conductive	
U20 R30	71.37 ± 3.16	44.80 ± 4.35	67.23 ± 0.86	36.29	23.21	40.51	12.30
U20 R60	56.21 ± 1.22	58.46 ± 2.54	69.90 ± 1.93	47.20	11.21	41.59	11.02
U20 R90	57.39 ± 0.63	69.48 ± 1.23	–	67.80	32.20	0.00	4.59
U27 R30	91.67 ± 0.47	60.04 ± 3.83	39.15 ± 3.88	42.26	13.90	43.85	8.17
U27 R60	91.01 ± 1.04	70.36 ± 3.64	50.38 ± 3.62	30.91	9.70	59.39	14.66
U27 R90	88.40 ± 0.68	62.40 ± 0.85	19.60 ± 0.42	50.67	34.67	14.67	18.89
U35 R30	90.43 ± 1.64	82.39 ± 0.88	50.41 ± 1.33	23.26	6.20	70.54	6.16
U35 R60	91.81 ± 0.40	82.28 ± 1.98	38.45 ± 1.75	35.78	11.01	53.21	18.25
U35 R90	89.10 ± 1.36	76.13 ± 2.61	11.87 ± 0.88	64.60	3.54	31.86	11.94

U – Voltage; R – Rotation.

Table 4
Characterization and mass distribution of the final fractions.

Metals	Concentration, %							Mass Distribution, %							
	Initial	> 0.5		0.5 > 0.25		< 0.25		> 0.5		0.5 > 0.25		< 0.25		**Total**	
		C	NC	C	NC	C	NC	C	NC	C	NC	C	NC	**C**	**NC**
Ag	**0.12**	0.02	0.03	0.03	0.03	0.39	0.01	3.31	0.93	1.53	3.78	89.38	1.07	**94.22**	**5.78**
Cu	**65.03**	98.75	3.08	90.13	2.69	82.88	9.29	39.49	0.23	11.10	0.82	45.96	2.41	**96.55**	**3.45**
Ga	**0.17**	0.00	0.08	0.00	0.36	0.02	0.62	0.00	2.10	0.00	38.18	3.85	55.87	**3.85**	**96.15**
Au	**0.06**	0.00	0.03	0.00	0.06	0.15	0.00	0.00	2.18	0.00	17.64	80.18	0.00	**80.18**	**19.82**
Sn	**4.26**	1.09	0.20	8.44	0.41	7.03	0.95	7.57	0.26	18.04	2.17	67.68	4.28	**93.29**	**6.71**
Ce	**0.01**	0.00	0.00	0.00	0.01	0.00	0.03	0.00	0.00	0.00	28.17	0.00	71.83	**0.00**	**100**
Y	**0.36**	0.00	0.10	0.01	0.17	0.04	1.56	0.00	1.55	0.25	10.64	4.55	83.00	**4.80**	**95.20**
Co	**ND**	ND	ND	ND	ND	ND	ND	–	–	–	–	–	–	–	–
Sb	**ND**	ND	ND	ND	ND	ND	ND	–	–	–	–	–	–	–	–
In	**ND**	ND	ND	ND	ND	ND	ND	–	–	–	–	–	–	–	–

C – Conductive Fraction; NC – Non Conductive Fraction; ND – Not Detected.

ICP-OES analysis (approximately 11%) and in the XRF analysis (approximately 12%).

The fraction C of the particle size > 0.5 is mainly composed of copper (98.75%). Tin is also present, with 1.09%, but such a concentration may not be relevant because it is lower than the initial LED concentration, and represents only 7.57% of the total tin, and the typical concentration of the tin natural ores is around 2% (Cenci et al., 2020b; Robben et al., 2020). The NC fraction of the particle size > 0.5 does not contain a significant amount of any element, excepting approximately 3% of copper. Thus, for the particle size > 0.5, copper is the most interesting material for recycling, with a concentration of 98.75% after electrostatic separation. These results indicate that particle size separation may be valuable for a recycling route, and the entire fraction (particle size > 0.5) has a conclusive destination: copper recovery.

After electrostatic separation, the C fraction of the particle size 0.5 > 0.25 was composed of 90.13% of copper and 8.44% of tin, corresponding to 11.10% of the total copper and 18.04% of the total tin. The NC fraction segregated and concentrated the critical element gallium, with 38.18% of the total amount of the final fractions. This concentration is two times higher than the initial LED concentration. There is also an amount of cerium and yttrium in the NC fraction (28.17% and 10.64% of the total mass, respectively), but with a lower concentration than the initial LEDs. The presence of gold and silver in the NC fraction may indicate that, in the particle size 0.5 > 0.25, the materials are not completely liberated since the electrical connections of gold and silver are involved with the light converting materials and polymers.

In particle size < 0.25, the C fraction still contained copper and tin (concentration of 82.88% and 7.03%, respectively), and now with significant amounts of silver and gold (89.38% of the total silver and 80.18% of the total gold of the final fractions). The amount of gold and silver in the final fraction are 2.5 and 3.3 times more concentrated than in the initial LEDs, and such concentrations of gold and silver are approximately, 75 and 6.5 times higher than the typical concentration of natural ores (Cenci et al., 2020b; Frimmel, 2018). These results, demonstrating the concentration of gold and silver in particle size < 0.25, support the use of particle size separation as a step of a recycling route. Gold and silver are employed, in the LED manufacturing, mainly as small solders and electric contacts for chips (exemplified in Fig. 1). Thus, the previous small dimensions of the components made of gold and silver resulted in these materials falling in the smaller fractions. Other metallic materials, such as copper and tin, which are present as larger components (larger solders and electric contacts), resulted in well distribution between all three fractions. The NC fraction contained most of the final amounts of gallium, cerium, and yttrium (55.87% of the total gallium, 71.83% of the total cerium and 83% of the total yttrium). This fraction compared with the initial LEDs, contains a higher concentration of 3.44 times for gallium, 3 times for cerium and 5.57 times for yttrium. The element gallium is utilized in the chips manufacturing as a layer above a piece of alumina (Al_2O_3). This component has a fragile behavior, being easily comminuted and falling into the smaller particle size fractions. As the chips also contain gold and silver, the fragile behavior may also contribute to their presence in the smallest particle size fraction. Thus, the particle size < 0.25 segregated and concentrated the valuable materials silver, copper, tin and gold in the C fraction, and the critical elements gallium, cerium, and yttrium in the NC fraction.

In general terms, the electrostatic separation segregated copper, tin, gold, and silver in the C fractions, and gallium, cerium, and yttrium in the NC fractions. The particle size separation was useful for segregating and concentrating elements, such as gold and silver at the particle size < 0.25 and indicating the destination of the particle size > 0.5 for copper recovery. According to the above results and discussion, it is possible to determine priority fractions per each target element for recycling, as shown in Table 5.

The physical processes proposed in this study, segregated, and concentrated valuable materials in mass and economic aspects (copper, tin, gold and silver) in the C fractions, and strategic critical elements in the NC fractions (gallium, cerium and yttrium). These physical processes allow different recycling strategies to be applied to each fraction, being useful to improve current recycling processes and discover new recycling alternatives. The gallium and REEs, that were indeed lost in the Reuter and Van Schaik (2015) simulations, could then be separately processed to recovery, the importance of which is emphasized by Ueberschaar et al. (2017) and Zhang et al. (2017).

3.4. Mass balance and efficiency of the proposed route

The characterization of the final fractions and the selection of the priority fraction for each element, analyzed in the section 3.3, demonstrated that the proposed route was effective in the separa-

Table 5
Priority fractions per each element for recycling.

Elements	Priority Fractions	
	Particle Size	Electrostatic Fraction
Silver (Ag)	< 0.25	Conductive
Copper (Cu)	All	Conductive
Gallium (Ga)	0.5 > 0.25 and < 0.25	Non Conductive
Gold (Au)	< 0.25	Conductive
Tin (Sn)	0.5 > 0.25 and < 0.25	Conductive
Cerium (Ce)	< 0.25	Non Conductive
Yttrium (Y)	< 0.25	Non Conductive

tion of valuable and critical materials. However, to analyze the overall efficiency of the route it is useful to provide a mass balance in which the total recovery for each element can be evaluated. Fig. 4 shows the materials balance of the particle size and electrostatic separation steps, with the mass amount per each element in both the initial LEDs and in the final fractions. The bold arrows represent the loss of mass in each step.

The loss of mass of the entire route was 11.81%. Most of the mass loss was generated in the milling and particle size separation, and in the electrostatic separation of the fraction < 0.25 (91.39%). By contrast, the mass losses in the electrostatic separation of the fractions > 0.5 and 0.5 > 0.25 was not significant, indicating a relation between a smaller particle size and higher loss of mass in the electrostatic separation. The higher loss of mass in the particle size < 0.25 is associated with dust generation in the processing of small particles (Schneider et al., 2019). Table 6 shows the efficiency parameters for evaluation of the proposed route. Mass loss, recovery rate (amount of material which reached the final priority fraction comparing with initial LEDs amounts) and concentration enhancement (concentration of the final priority fractions comparing with initial LEDs concentration) were calculated per element.

According to Jiang et al. (2012), the steps of milling and particle size separation alone could lead to up to 40% of material loss. Indeed, the material loss was found to be a significant limiting factor for the proposed route in which the elements tin and yttrium had losses of approximately 30%, and>20% for copper. Silver, gold, and gallium were the elements that suffered lower losses (5.63%, 9.09% and 13.45%, respectively). The loss of mass negatively impacted the recovery rate of the elements: <60% of the total amount of tin and yttrium reached the final priority fractions. However, significant recovery rates were still achieved, such as 85.53% for silver, 81.20% for gallium, and 76.23% for copper.

Table 6
Efficiency parameters of the route per element.

Elements	Mass Loss (%)	Priority Fractions Recovery (%)	Concentration Enhancement in the Priority Fractions (%)
Silver (Ag)	5.63	85.53	325
Copper (Cu)	21.03	76.23	127–152
Gallium (Ga)	13.45	81.20	212–365
Gold (Au)	9.09	71.97	250
Tin (Sn)	30.43	59.60	165–198
Cerium (Ce)	18.53	70.00	306
Yttrium (Y)	30.28	57.68	433

Despite the limitations imposed by the loss of materials, the proposed route effectively segregated the valuable and critical elements into different fractions (conductive and non-conductive) and concentrated them in the priority fractions, as can be seen in Table 4 and Table 6. Yttrium was concentrated>400%, cerium, gallium and silver>300%, gold>200%, and copper and tin>100%.

3.5. Destination suggestions for the final fractions

The proposed route is useful as an initial step of a recycling route. After the segregation and concentration of the valuable and critical materials, methods of extractive metallurgy may be applied on the final fractions to complete the recycling.

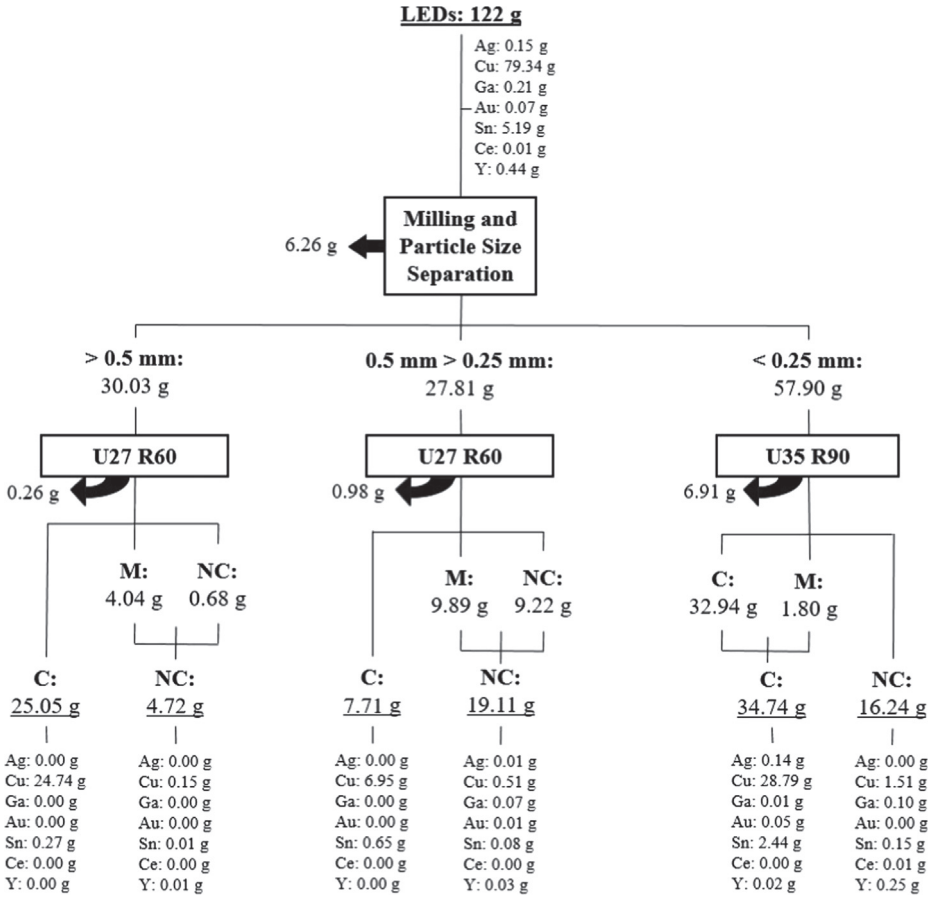

Fig. 4. Mass balance of the proposed route.

The conductive fraction of the particle size > 0.5 is almost totally composed of copper, with a small amount of tin (approximately 1%). Copper recovery is the conclusive destination of this fraction. The copper smelting process is established as one of the main recycling alternatives for several WEEE and may be also applied for this LED's fraction. Primary or secondary copper smelting and their associated refinement structures are able to process a wide range of inputs, and produce high quality materials from the dissolved elements (Avarmaa et al., 2018; Reuter and Van Schaik, 2015). The treatment given to the residue depends on its purity, in which lower grade materials are smelted and refined, and higher grade materials can be directly fire refined and electro-refined (Schlesinger et al., 2011). It is important to highlight that high quality materials can be melted and cast without refining, and used as non-electrical products, such as tube, sheet and alloys (brass, bronze) (Schlesinger et al., 2011). Due to the low concentration of impurities (approximately 100% of copper and tin), this fraction is possible to skip the refining or smelting steps. Such an opportunity needs to be further studied.

The non-conductive fraction of the particle size > 0.5 still contains approximately 3% of copper, which is slightly more than typical primary ore's concentration (2.52 – 2.78%) (Cenci et al., 2020b). Thus, recovery of copper is also an alternative destination for this fraction, as a low grade material input into the smelting process. Note that the electrostatic separation for the particle size > 0.5 is only convenient if the C and NC fractions have different destinations. If both C and NC fraction have the same destination (copper smelting process), only particle size separation is suggested.

Copper and tin are the main constituents of the C fraction of the particle size 0.5 > 0.25 (90% and 8%, respectively). The same alternatives discussed for the C fraction of the particle size > 0.5 apply to the particle size 0.5 > 0.25, as this fraction has the potential to be considered high quality scrap. This fraction contains a similar composition to bronze alloys (copper and tin), and can be further studied to consider its similarity to bronze scraps in recycling. Some slagging can be produced to remove contaminants, and there would be no advantage in smelting or refining the fraction to pure copper (Schlesinger et al., 2011).

Gallium was segregated and concentrated in the NC fraction of the particle size 0.5 > 0.25 (0.36%). All the gallium is present in the form of gallium nitride, which is highly resistant to chemical leaching (Zhuang and Edgar, 2005). Some authors proposed complete pyrometallurgical solutions, or hydrometallurgical methods after a pyrometallurgical step. The route utilized by Zhou et al. (2019), comprising organic acid leaching after pyrolysis, for concentration and decomposition of the gallium nitride, seems promising. Hydrometallurgical methods for extraction of the remaining copper (concentration of approximately 2.7%), prior to the processing of gallium, is suggested as an opportunity to improve the overall recovery of LEDs materials.

The C fraction of the particle size < 0.25 segregated and concentrated the valuable materials gold, silver, copper, and tin. Ideally, all of them may be recovered. Alternative hydrometallurgical routes are suggested due to their potential to be selective and effective. Indeed, the concentration provided by the particle size and electrostatic separation may improve their recovery efficiency and facilitate the process. Dong et al. (2020) proposed a hydrometallurgical route to selectively recover copper, gold and silver through different chemical leaching agents, similar alternatives may be further studied.

The NC fraction of the particle size < 0.25 requires further study to have its critical materials recovered. Indeed, one of the main objectives of this study was to enhance the concentration of gallium, yttrium, and cerium to allow more effective and efficient recycling alternatives. Due to the nature of the substances where these elements are found (GaN and Ce:$Y_3Al_5O_{12}$), pyro and hydrometallurgical methods are suggested to be utilized together. Particularly, the recycling behavior of the yttrium–aluminum garnet needs to be further investigated.

4. Conclusions

This study proposed the use of physical processes (particle size and electrostatic separation) for separating and concentrating wasted LED materials, as a first step of a recycling route. It was expected that valuable elements, such as gold, silver, copper, and tin, would become concentrated in the conductive fractions, and the critical elements gallium and REEs become concentrated in the non-conductive fractions. This expectation was successfully achieved. Electrostatic separation was effective in separating and concentrating critical strategic materials from economic valuable materials, into different conductive and non-conductive fractions, and particle size separation had an important role in concentrating such materials in specific granulometries. Gallium and REEs were mainly found in the non-conductive fractions of the particle sizes 0.5 > 0.25 mm and < 0.25 mm (96.15% of the total gallium, 100% of the cerium, and 95.20% of the total yttrium in non-conductive fractions), and in the conductive fractions, we highlight gold and silver, which were mainly concentrated in the particle size < 0.25 mm (80.18% of the total gold and 89.38% of the total silver). Copper and tin also became segregated and concentrated in the conductive fractions (96.55% and 93.29% of the total mass, respectively). The concentration of valuable and critical materials was enhanced from 127% for copper up to 433% for yttrium.

Despite the success in separating and concentrating the materials, the loss of mass is a limiting factor for the route efficiency, as it was significant for some elements and impacted their recovery rates. The loss of mass of the entire route was approximately 12%. Tin and yttrium were the most affected elements, with approximately 30% of mass loss, and gold and silver the less affected, with approximately 9% and 6%, respectively. However, for further applications, even on an industrial scale, this loss of mass can be minimized at some level by technology advances, more robust equipment, operational refinement, and further studies.

The proposed route valorized the residue and may enable nobler destination alternatives for it. High quality fractions were generated which may facilitate the posterior processing in recycling facilities. Conductive fractions composed of copper may skip the smelting step of the recycling route and be processed directly into the refining steps or serve as an input material for alloy casting (such as for bronze). The provided concentration enhancement of critical materials may uncover new alternatives, and improve the current alternatives for their recycling, as the low concentration is a significant limiting factor as pointed out by several researchers. Indeed, more studies are needed to define recycling strategies for them. Additionally, the achieved material's segregation and concentration may be relevant to the economic viability of the recycling routes, highlighting that economic and strategic aspects are the main driving forces leading to investments in the field.

Declaration of Competing Interest

The authors declared that there is no conflict of interest.

Acknowledgment

This research is supported by the CAPES – Coordenação de Aperfeiçoamento de Pessoal de Nível Superior (CAPES/ PROEX 23038.000341/2019-71 0491/2019) and the others Brazilian government agencies CNPq, Finep and Fapergs.

Appendix A. Supplementary data

Supplementary data to this article can be found online at https://doi.org/10.1016/j.wasman.2020.11.023.

References

Avarmaa, K., Yliaho, S., Taskinen, P., 2018. Recoveries of rare elements Ga, Ge, In and Sn from waste electric and electronic equipment through secondary copper smelting. Waste Manage. 71, 400–410. https://doi.org/10.1016/j.wasman.2017.09.037.

Baldé, C.P., Forti, V., Gray, V., Kuehr, R., Stegmann, P., 2017. The global E-waste Monitor - 2017, United Nations University (UNU), International Telecommunication Union (ITU) & International Solid Waste Association (ISWA). Bonn/Geneva/Vienna.

Cenci, M.P., Dal Berto, F.C., Castillo, B.W., Veit, H.M., 2020. Precious and Critical Metals from Wasted LED Lamps: Characterization and Evaluation. Environ. Technol. https://doi.org/10.1080/09593330.2020.1856939. In press.

Cenci, M.P., Dal Berto, F.C., Schneider, E.L., Veit, H.M., 2020. Assessment of LED lamps components and materials for a recycling perspective. Waste Manage. 107, 285–293. https://doi.org/10.1016/j.wasman.2020.04.028.

Cho, J., Park, J.H., Kim, J.K., Schubert, E.F., 2017. White light-emitting diodes: History, progress, and future: White light-emitting diodes. Laser Photonics Rev. 11 (2), 1600147. https://doi.org/10.1002/lpor.201600147.

Clarke, C., Williams, I.D., Turner, D.A., 2019. Evaluating the carbon footprint of WEEE management in the UK. Resour. Conserv. Recycl. 141, 465–473. https://doi.org/10.1016/j.resconrec.2018.10.003.

David, A., Whitehead, L.A., 2018. LED-based white light. C.R. Phys. 19 (3), 169–181. https://doi.org/10.1016/j.crhy.2018.02.004.

Deubzer, O., Jordan, R., Marwede, M., Chancerel, P., 2012. Categorization of LED products.

Dong, Z., Jiang, T., Xu, B., Yang, J., Chen, Y., Li, Q., Yang, Y., 2020. Comprehensive recoveries of selenium, copper, gold, silver and lead from a copper anode slime with a clean and economical hydrometallurgical process. Chem. Eng. J. 393, 124762. https://doi.org/10.1016/j.cej.2020.124762.

Dzombak, R., Antonopoulos, C., Dillon, H.E., 2019. Balancing technological innovation with waste burden minimization: An examination of the global lighting industry. Waste Manage. 92, 68–74. https://doi.org/10.1016/j.wasman.2019.04.037.

European Commission, 2020. Communication from the commission to the European Parliament, the Council, the European Economic and Social Committee and the Committee of the Regions: A new circular economy action plan for a cleaner and more competitive Europe [WWW Document]. URL https://eur-lex.europa.eu/legal-content/EN/TXT/?qid=1585833760031&uri=CELEX:52020DC0098 (accessed 4.2.20).

European Commission, 2018. Report on critical raw materials and the circular economy. https://doi.org/10.2873/167813.

Fang, S., Yan, W., Cao, H., Song, Q., Zhang, Y.i., Sun, Z., 2018. Evaluation on end-of-life LEDs by understanding the criticality and recyclability for metals recycling. J. Cleaner Prod. 182, 624–633. https://doi.org/10.1016/j.jclepro.2018.01.260.

Feezell, D., Nakamura, S., 2018. Invention, development, and status of the blue light-emitting diode, the enabler of solid-state lighting. C.R. Phys. 19 (3), 113–133. https://doi.org/10.1016/j.crhy.2017.12.001.

Franz, M., Wenzl, F.P., 2017. Critical review on life cycle inventories and environmental assessments of LED-lamps. Critical Rev. Environ. Sci. Technology 47 (21), 2017–2078. https://doi.org/10.1080/10643389.2017.1370989.

Frimmel, H.E., 2018. Episodic concentration of gold to ore grade through Earth's history. Earth Sci. Rev. 180, 148–158. https://doi.org/10.1016/j.earscirev.2018.03.011.

Gayral, B., 2017. LEDs for lighting: Basic physics and prospects for energy savings. C. R. Phys. 18 (7-8), 453–461. https://doi.org/10.1016/j.crhy.2017.09.001.

Grigoropoulos, C.J., Doulos, L.T., Zerefos, S.C., Tsangrassoulis, A., Bhusal, P., 2020. Estimating the benefits of increasing the recycling rate of lamps from the domestic sector: Methodology, opportunities and case study. Waste Manage. 101, 188–199. https://doi.org/10.1016/j.wasman.2019.10.010.

Hadi, P., Xu, M., Lin, C.S.K., Hui, C.-W., McKay, G., 2015. Waste printed circuit board recycling techniques and product utilization. J. Hazard. Mater. 283, 234–243. https://doi.org/10.1016/j.jhazmat.2014.09.032.

Hamerski, F., Bernardes, D.P., Veit, H.M., 2018. Operational conditions of an electrostatic separator for concentrate copper from electronic waste. Rem Int. Eng. J. 71, 431–436. https://doi.org/10.1590/0370-44672017710159.

Heiberger, R.M., Holland, B., 2009. Statistical Analysis and Data Display, 2nd ed, Springer, Springer Texts in Statistics. https://doi.org/10.1007/978-1-4757-4284-8.

Hoffman, J.I.E., 2019. Basic Biostatistics for Medical and Biomedical Practitioners. Elsevier, 391–417. https://doi.org/10.1016/B978-0-12-817084-7.00025-5.

Hunt, A.M.W., Speakman, R.J., 2015. Portable XRF analysis of archaeological sediments and ceramics. J. Archaeol. Sci. 53, 626–638. https://doi.org/10.1016/j.jas.2014.11.031.

Ilankoon, I.M.S.K., Ghorbani, Y., Chong, M.N., Herath, G., Moyo, T., Petersen, J., 2018. E-waste in the international context – A review of trade flows, regulations, hazards, waste management strategies and technologies for value recovery. Waste Manage. 82, 258–275. https://doi.org/10.1016/j.wasman.2018.10.018.

Işıldar, A., Rene, E.R., van Hullebusch, E.D., Lens, P.N.L., 2018. Electronic waste as a secondary source of critical metals: Management and recovery technologies. Resour. Conserv. Recycl. 135, 296–312. https://doi.org/10.1016/j.resconrec.2017.07.031.

Jiang, P., Harney, M., Song, Y., Chen, B., Chen, Q., Chen, T., Lazarus, G., Dubois, L.H., Korzenski, M.B., 2012. Improving the End-of-Life for Electronic Materials via Sustainable Recycling Methods. Procedia Environ. Sci. 16, 485–490. https://doi.org/10.1016/j.proenv.2012.10.066.

Kaya, M., 2016. Recovery of metals and nonmetals from electronic waste by physical and chemical recycling processes. Waste Manage. 57, 64–90. https://doi.org/10.1016/j.wasman.2016.08.004.

Kumar, A., Kuppusamy, V.K., Holuszko, M., Song, S., Loschiavo, A., 2019. LED lamps waste in Canada: Generation and characterization. Resour. Conserv. Recycl. 146, 329–336. https://doi.org/10.1016/j.resconrec.2019.04.006.

Lim, S.-R., Kang, D., Ogunseitan, O.A., Schoenung, J.M., 2011. Potential Environmental Impacts of Light-Emitting Diodes (LEDs): Metallic Resources, Toxicity, and Hazardous Waste Classification. Environ. Sci. Technol. 45 (1), 320–327. https://doi.org/10.1021/es101052q.

Murakami, H., Nishihama, S., Yoshizuka, K., 2015. Separation and recovery of gold from waste LED using ion exchange method. Hydrometallurgy 157, 194–198. https://doi.org/10.1016/j.hydromet.2015.08.014.

Murali, K.V.R.M., Naik, V.B., Datta, D., 2015. Gallium-nitride-based light-emitting diodes: 2014 Nobel Prize in Physics. Reson 20 (7), 605–616. https://doi.org/10.1007/s12045-015-0219-y.

Nagy, S., Bokányi, L., Gombkötő, I., Magyar, T., 2017. Recycling of Gallium from End-of-Life Light Emitting Diodes. Arch. Metall. Mater. 62 (2), 1161–1166. https://doi.org/10.1515/amm-2017-0170.

Ogunseitan, O.A., Schoenung, J.M., Saphores, J.-D.- M., Shapiro, A.A., 2009. The Electronics Revolution: From E-Wonderland to E-Wasteland. Science 326 (5953), 670–671. https://doi.org/10.1126/science:1176929.

Petter, P.M.H., Veit, H.M., Bernardes, A.M., 2014. Evaluation of gold and silver leaching from printed circuit board of cellphones. Waste Manage. 34 (2), 475–482. https://doi.org/10.1016/j.wasman.2013.10.032.

Radu, T., Diamond, D., 2009. Comparison of soil pollution concentrations determined using AAS and portable XRF techniques. J. Hazard. Mater. 171 (1-3), 1168–1171. https://doi.org/10.1016/j.jhazmat.2009.06.062.

Zamprogno Rebello, R., Weitzel Dias Carneiro Lima, M.T., Yamane, L.H., Ribeiro Siman, R., 2020. Characterization of end-of-life LED lamps for the recovery of precious metals and rare earth elements. Resour. Conserv. Recycl. 153, 104557. https://doi.org/10.1016/j.resconrec.2019.104557.

Reuter, M.A., van Schaik, A., 2015. Product-Centric Simulation-Based Design for Recycling: Case of LED Lamp Recycling. J. Sustain. Metall. 1 (1), 4–28. https://doi.org/10.1007/s40831-014-0006-0.

Richard, G., Touhami, S., Zeghloul, T., Dascalescu, L., 2017. Optimization of metals and plastics recovery from electric cable wastes using a plate-type electrostatic separator. Waste Manage. 60, 112–122. https://doi.org/10.1016/j.wasman.2016.06.036.

Robben, C., Condori, P., Pinto, A., Machaca, R., Takala, A., 2020. X-ray-transmission based ore sorting at the San Rafael tin mine. Miner. Eng. 145, 105870. https://doi.org/10.1016/j.mineng.2019.105870.

Ruiz-Mercado, G.J., Gonzalez, M.A., Smith, R.L., Meyer, D.E., 2017. A conceptual chemical process for the recycling of Ce, Eu, and Y from LED flat panel displays. Resour. Conserv. Recycl. 126, 42–49. https://doi.org/10.1016/j.resconrec.2017.07.009.

Scheff, S.W., 2016. Fundamental Statistical Principles for the Neurobiologist. Elsevier, 97–133. https://doi.org/10.1016/B978-0-12-804753-8.00006-3.

Schlesinger, M.E., King, M.J., Sole, K.C., Davenport, W.G., 2011. Extractive Metallurgy of Copper, 5th ed, Dk. Elsevier. https://doi.org/10.1017/CBO9781107415324.004.

Schneider, E.L., Hamerski, F., Veit, H.M., Krummenauer, A., Cenci, M.P., Chaves, R.D. A., Hartmann, W.L., Dias, M.D.M., Robinson, L.C., Vargas, A.S.D., 2019. Evaluation of mass loss in different stages of printed circuit boards recycling employed in temperature controllers. Mater. Res. 22,. https://doi.org/10.1590/1980-5373-mr-2018-0833 e20180833.

Swain, B., Mishra, C., Kang, L., Park, K.-S., Lee, C.G., Hong, H.S., 2015a. Recycling process for recovery of gallium from GaN an e-waste of LED industry through ball milling, annealing and leaching. Environ. Res. 138, 401–408. https://doi.org/10.1016/j.envres.2015.02.027.

Swain, B., Mishra, C., Kang, L., Park, K.-S., Lee, C.G., Hong, H.S., Park, J.-J., 2015b. Recycling of metal-organic chemical vapor deposition waste of GaN based power device and LED industry by acidic leaching: Process optimization and kinetics study. J. Power Sources 281, 265–271. https://doi.org/10.1016/j.jpowsour.2015.01.189.

Swain, B., Mishra, C., Lee, K.-J., Hong, H.S., Park, K.-S., Lee, C.G., 2016. Recycling of GaN, a Refractory eWaste Material: Understanding the Chemical Thermodynamics. Int. J. Appl. Ceram. Technol. 13 (2), 280–288. https://doi.org/10.1111/ijac.12473.

Ueberschaar, M., Otto, S.J., Rotter, V.S., 2017. Challenges for critical raw material recovery from WEEE – The case study of gallium. Waste Manage. 60, 534–545. https://doi.org/10.1016/j.wasman.2016.12.035.

UNEP, 2017. Accelerating the Global Adoption of Energy-Efficient Lighting [WWW Document]. URL https://united4efficiency.org/resources/accelerating-global-adoption-energy-efficient-lighting/ (accessed 8.27.19).

Veit, H.M., Diehl, T.R., Salami, A.P., Rodrigues, J.S., Bernardes, A.M., Tenório, J.A.S., 2005. Utilization of magnetic and electrostatic separation in the recycling of printed circuit boards scrap. Waste Manage. 25 (1), 67–74. https://doi.org/10.1016/j.wasman.2004.09.009.

Yamane, L.H., de Moraes, V.T., Espinosa, D.C.R., Tenório, J.A.S., 2011. Recycling of WEEE: Characterization of spent printed circuit boards from mobile phones and computers. Waste Manage. 31 (12), 2553–2558. https://doi.org/10.1016/j.wasman.2011.07.006.

Zhan, L.u., Xia, F., Ye, Q., Xiang, X., Xie, B., 2015. Novel recycle technology for recovering rare metals (Ga, In) from waste light-emitting diodes. J. Hazard. Mater. 299, 388–394. https://doi.org/10.1016/j.jhazmat.2015.06.029.

Zhang, L., Xu, Z., 2016. A review of current progress of recycling technologies for metals from waste electrical and electronic equipment. J. Cleaner Prod. 127, 19–36. https://doi.org/10.1016/j.jclepro.2016.04.004.

Zhang, S., Ding, Y., Liu, B.o., Chang, C.-C., 2017. Supply and demand of some critical metals and present status of their recycling in WEEE. Waste Manage. 65, 113–127. https://doi.org/10.1016/j.wasman.2017.04.003.

Zhou, J., Zhu, N., Liu, H., Wu, P., Zhang, X., Zhong, Z., 2019. Recovery of gallium from waste light emitting diodes by oxalic acidic leaching. Resour. Conserv. Recycl. 146, 366–372. https://doi.org/10.1016/j.resconrec.2019.04.002.

Zhuang, D., Edgar, J.H., 2005. Wet etching of GaN, AlN, and SiC: a review. Materials Science and Engineering: R: Reports 48 (1), 1–46. https://doi.org/10.1016/j.mser.2004.11.002.

Zissis, G., Bertoldi, P., 2018. Status of LED-Lighting world market in 2017. European Commission, Ispra.